Miniemulsion Copolymerizations of Styrene and Reactive Alkyl Methacrylate Costabilizers

C.T. Lin Kusdianto, F.E. Yu, C.S. Chern

Department of Chemical Engineering, National Taiwan University of Science and Technology, Taipei, 106 Taiwan

Received 11 February 2010; accepted 26 April 2010
DOI 10.1002/app.32718
Published online 27 July 2010 in Wiley Online Library (wileyonlinelibrary.com).

ABSTRACT: Miniemulsion copolymerizations of styrene (ST) and stearyl methacrylate (SMA) or lauryl methacrylate (LMA) were investigated. Miniemulsions comprising ST and various levels of SMA showed very good storage stability against the diffusional degradation of monomer droplets (Ostwald ripening), whereas miniemulsions comprising ST and various levels of LMA exhibited significant Ostwald ripening. In subsequent miniemulsion copolymerizations of ST and SMA, particle nucleation occurring in the continuous aqueous phase (homogeneous nucleation) plays an important role in the particle formation process in addition to monomer droplet nucleation. The final overall conversion and the individual conversions of ST and SMA all decrease with increasing SMA concentration. Furthermore, at a particular reaction time, the individual conversion of SMA is always greater than that of ST. Monomer droplet nucleation was retarded severely for the monomer pair ST/LMA, presumably due to the very strong Ostwald ripening effect. As a result, relatively slow rates of copolymerization of ST and LMA were attained compared with the ST/SMA counterpart. © 2010 Wiley Periodicals, Inc. J Appl Polym Sci 119: 620–628, 2011

Key words: miniemulsion copolymerization; styrene; alkyl methacrylates; Ostwald ripening

INTRODUCTION

Oil in water emulsions stabilized by anionic and/or nonionic surfactants against coalescence are colloidal systems, in which oil droplets with a relatively broad droplet size distribution are dispersed in the continuous aqueous phase.[1] These classic emulsions are thermodynamically unstable because of the very large oil-water interfacial free energy. Higuchi and Misra[2] were the first to illustrate that addition of a small amount of a water-insoluble compound (termed costabilizer) would retard the degradation of emulsions via the Ostwald ripening process (i.e., oil molecules in small droplets tend to diffuse through the continuous aqueous phase into large ones, and thus, large droplets grow in size at the expense of small ones). This was followed by some representative studies focusing on the fundamental aspects of Ostwald ripening in the presence of costabilizers.[3–6] The relatively stable products thus obtained are termed miniemulsions.

Polymerization of conventional monomer emulsions involves the generation and growth of particle nuclei via either micellar nucleation[7–12] or homogeneous nucleation.[13–17] Emulsified monomer droplets generally do not contribute to particle nucleation to any appreciable extent in emulsion polymerization because of their very small droplet surface area and, therefore, they only serve as monomer reservoir to supply growing particles with monomer according to the micellar nucleation mechanism. Nevertheless, homogenized monomer droplets containing a hydrophobic low molecular weight compound [e.g., hexadecane (HD) or cetyl alcohol (CA)] may become predominant particle nucleation loci provided that the total monomer droplet surface area becomes large enough to compete effectively with the aqueous phase, in which particle nuclei are generated, for capturing radicals (monomer droplet nucleation). This unique technique has been termed miniemulsion polymerization.[18–25]

Chern and co-workers[26–29] investigated miniemulsion polymerizations of ST using relatively low levels of alkyl methacrylates [stearyl methacrylate (SMA) and lauryl methacrylate (LMA)] as the reactive costabilizers. Just like conventional costabilizers, long-chain alkyl methacrylates act as costabilizers in stabilizing submicron monomer droplets against Ostwald ripening. Furthermore, the methacrylate group of the polymerizable costabilizer can be chemically incorporated into latex particles in the subsequent free radical polymerization. Recently, Chern et al.[30] prepared miniemulsion copolymers of ST and SMA in the range 20–50 wt %, and evaluated the water

Correspondence to: C.S. Chern (cschern@mail.ntust.edu.tw).

repellent property of the resultant copolymer films. X-ray photoelectron spectroscopy measurements showed that a concentration gradient of monomeric units of SMA within the polymeric film was established during film formation and the concentration of monomeric units of SMA was the highest within the surface layer. This implies that copolymer species with different compositions formed during polymerization, presumably due to a mixed mode of particle nucleation (monomer droplet nucleation and homogeneous nucleation) and the monomer pair ST/SMA with different reactivity ratios and solubility parameters.[30] To further verify this postulation, the objective of this work was therefore to gain a better understanding of the copolymerization kinetics and mechanisms for the two monomer pairs ST/SMA and ST/LMA.

EXPERIMENTAL

Materials

The chemicals used include ST (Taiwan Styrene), SMA (Aldrich), LMA (Aldrich, 95%), sodium lauryl sulfate (SLS, J. T. Baker, 99%), sodium persulfate (SPS, Riedel de Haen), and sodium bicarbonate (Riedel de Haen) as the buffer. Other reagents used include dichloromethane (Riedel de Haen), ethanol (95%), chloroform (Acros), toluene (Acros), pure nitrogen gas, and deionized water (Barnsted, Nanopure Ultrapure Water System, specific conductance < 0.057 μS/cm). SMA was recrystallized in ethanol, and ST distilled under reduced pressure before use. Other chemicals were used as received.

Preparation and characterization of miniemulsions

The miniemulsion was prepared by dissolving SLS and sodium bicarbonate in water and costabilizer (SMA or LMA) in ST, respectively. The oily and aqueous solutions were mixed using a mechanical agitator at 400 rpm for 10 min. The resultant emulsion was then homogenized with an ultrasonic homogenizer (Misonix sonicator 3000) for ten cycles of 5 min in length with 2 min off-time, and the output power set at 12 W. A typical miniemulsion formulation comprises the aqueous phase (160 g of water, 2.66 m*M* of sodium bicarbonate and 5 m*M* of SLS), the monomer charge (40 g of ST, kept constant in this study) and various amounts of costabilizers (SMA or LMA). The runs corresponding to the mass ratios of ST : SMA = 1 : 1, 2 : 1, and 4 : 1 were designated as S11, S21, and S41, respectively. The runs corresponding to the mass ratios of ST : LMA = 1 : 1, 2 : 1, 4 : 1, 8:1, 16 : 1, and 50.4 : 1 were designated as L11, L21, L41, L81, L161, and L501, respectively. The concentrations of sodium bicarbonate and SLS are based on the total water weight. The average monomer droplet diameter of miniemulsion upon aging was determined by dynamic light scattering (DLS, Malvern, Zetasizer 1000 HSA). The sample was diluted with water saturated with SLS and ST to avoid the multiple scattering of monomer droplets and the potential diffusion of SLS and ST species from droplets into the aqueous phase.

Miniemulsion polymerization

Immediately after homogenization, the resultant miniemulsion was charged into a 500-mL reactor equipped with a four-bladed fan turbine agitator, a thermocouple, and a reflux condenser and then purged with nitrogen for 10 min to remove dissolved oxygen, whereas the temperature was brought to 70°C. The initiator solution (2.66 m*M* of SPS based on total water weight) was then charged into the reactor to start the polymerization, and the temperature kept constant at 70°C throughout the reaction. The agitation speed was set at 400 and 800 rpm for the ST/SMA and ST/LMA system over a period of 8 h, respectively. A higher agitation speed for the ST/LMA system was used because appreciable phase separation of miniemulsion was observed when an agitation speed of 400 rpm was adopted in this series of experiments. The latex product was filtered through 40-mesh and 200-mesh screens in series. Scraps adhering to the agitator, thermometer and reactor wall were also collected. The average colloidal particle size during the reaction was determined by DLS.

Individual conversions of monomer and costabilizers

Individual conversions of ST and reactive costabilizer (SMA or LMA) were determined by the UV/visible spectrometer (Shimadzu UV-1061) and FTIR spectrometer (Bio-Rad FTS-3500), respectively. First, the dried copolymer sample was dissolved in dichloromethane, and the UV absorbance at 264 nm primarily originating from monomeric units of ST in the sample was determined based on a calibration curve obtained from pure polystyrene standards [absorbance = 2716.5 × concentration (g/g)]. The correction required to take into account the presence of costabilizer (SMA or LMA) as monomer molecules or monomeric units in the copolymer was made by measuring the UV absorbance of pure SMA [absorbance = 118.5 ×concentration (g/g)] or LMA [absorbance = 120.5×concentration (g/g)] at 264 nm in combination with a mass balance on SMA or LMA in the recipe. The individual conversion of SMA or LMA was then determined by the FTIR characteristic

peak area at 1635 1/cm for —C=C— of SMA or LMA according to a calibration curve obtained from pure SMA [peak area = 14,874 × concentration (g/g)] or LMA [peak area = 18,564 × concentration (g/g)].

RESULTS AND DISCUSSION

Stability of miniemulsions upon aging

The rate of Ostwald ripening (R_o) for the two-component disperse phase system can be calculated by the following equation based on the modified LSW theory[31]:

$$R_O = 1/8\ d\ (d_m{}^3)/d\ t = 8\sigma D_c V_m C_c(\infty)/(9RTv_c) \quad (1)$$

where d_m is the monomer droplet diameter, t the aging time, σ the droplet-water interfacial tension, D_c the molecular diffusivity of costabilizer in water, V_m the molar volume of monomer in the droplets, C_c (∞) the solubility of the bulk costabilizer in water, R the gas constant, T the absolute temperature, and v_c the volume fraction of costabilizer in the monomer droplets. Figure 1 shows the data of $d_m{}^3$ as a function of t for miniemulsions of ST stabilized by various levels of SMA or LMA at 30°C. The concentration of SLS was kept constant at 5 m*M* which is slightly below the critical micelle concentration (CMC, 8.2 m*M*).[32] Ostwald ripening does not occur eventually for the series of miniemulsions comprising ST and SMA, as shown in Figures 1(a) and 2. This is due to the fact that SMA is an extremely effective costabilizer and it can provide sufficient osmotic pressure to counterbalance the Laplace pressure (Ostwald ripening). On the other hand, the Ostwald ripening effect plays an important role in the stability of miniemulsions comprising ST and LMA, even for the runs with the weight fraction of LMA greater than 0.1 [Fig. 1(b,c)]. The Ostwald ripening rate first decreases and then levels off with increasing LMA concentration for the series of miniemulsions containing ST and LMA (Fig. 2). This is because LMA (water solubility 1.38 × 10^{-8} cm^3/cm^3) is less hydrophobic than SMA (water solubility ca. 3.23 × 10^{-9} cm^3/cm^3).[5] The higher the water solubility of costabilizer, the faster the Ostwald ripening rate, according to eq. (1). It should be noted that the rate of Ostwald ripening is inversely proportional to the absolute temperature [eq. (1)]. Thus, the Ostwald ripening rates of miniemulsions at the polymerization temperature) (70°C) are overestimated by a factor of ca. 12% compared with the reported Ostwald ripening rate data at 30°C. However, this factor is not expected to change the relative importance of the influence of the Ostwald ripening process on the particle nucleation mechanisms in the ST/SMA or ST/LMA copolymerization systems with different levels of the reactive alkyl methacrylate costabilizers.

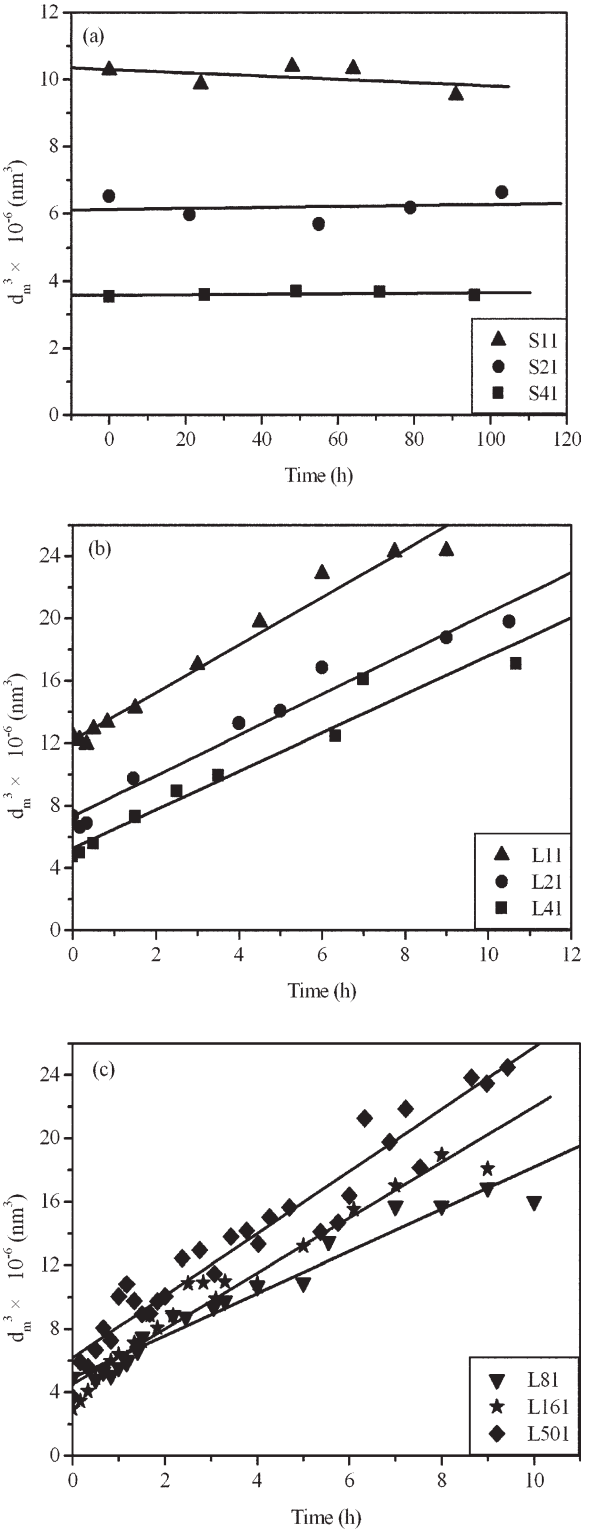

Figure 1 Cubic of average monomer droplet diameter as a function of time for miniemulsions upon aging at 30°C prepared by various mass ratios of ST : SMA or ST : LMA. (a) (▲) S11, (●) S21, (■) S41; (b) (▲) L11, (●) L21, (■) L41; (c) (▼) L81, (★) L161, (◆) L501.

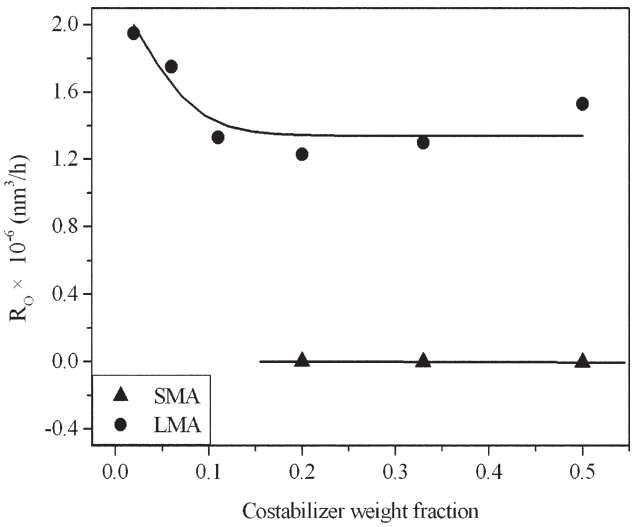

Figure 2 Ostwald ripening rate as function of costabilizer weight fraction [costabilizer/(ST + costabilizer) (w/w)] for miniemulsions upon aging at 30°C. (▲) SMA, (●) LMA.

Miniemulsion copolymerization mechanisms and kinetics

The recipes and experimental data for miniemulsion copolymerizations of ST with various levels of SMA and LMA are summarized in Table I. In this study, the concentrations of SLS and SPS and the amounts of ST and water were kept constant at 5 m*M*, 2.66 m*M*, and 40 g and 160 g, respectively. Both the individual conversions of ST and SMA are shown in Figure 3. It is shown that the polymerization rate of SMA is much faster than that of ST in this series of experiments. Furthermore, the difference in the polymerization rate becomes greater when the amount of SMA increases. For illustration, the rate of polymerization for the miniemulsion polymerization in the presence of conventional costabilizer (e.g., HD and CA) can be expressed as follows:

$$R_p = k_p[M]_p n N_p / N_A \quad (2)$$

where k_p is the propagation rate constant, $[M]_p$ the concentration of monomer in the particles, n the average number of free radicals per particle, N_p the number of latex particles per unit volume of water, and N_A the Avogadro number. eq. (2) predicts that the rate of polymerization is linearly proportional to nN_p and k_p. First, at a particular reaction time, the average size (d) of colloid particles (including monomer-swollen polymer particles and unnucleated monomer droplets) decreases with increasing weight fraction of SMA (Fig. 4). This is because the more hydrophobic colloidal particles that contain more SMA molecules require more SLS species adsorbed on their surfaces to achieve adequate colloidal stability. As a result, the number of latex particles (i.e., reaction loci) decreases with increasing weight fraction of SMA during polymerization, as demonstrated by the final number of latex particles per unit volume of water ($N_{p,f}$) data for the runs S41, S21, and S11 in Table I. For the ST/SMA series of experiments, it is very difficult to estimate n directly from eq. (2) due to the lack of the propagation rate constant data for SMA and the concentrations of the individual comonomers ST and SMA in the polymer particles originating from the monomer droplet nucleation and homogeneous nucleation mechanisms. With the assumption of negligible desorption of free radicals out of the latex particles (a reasonable assumption for the copolymerization systems containing the hydrophobic monomer pairs ST/SMA and ST/LMA), the following relationship can be used to estimate n.[33]

$$n = (0.25 + \alpha'/2)^{1/2} \quad (3)$$

where the dimensionless group α' is defined as $\rho_i \bar{v}_p / k_{tp} N_p$, $\rho_i = 2fk_d[I]_w$ is the rate of generation of free

TABLE I
Recipes and Some Experimental Data Obtained from Miniemulsion Copolymerizations of St and SMA or LMA

	S41	S21	S11	L501	L161	L81	L41	L21	L11
ST/costabilizer (w/w)	40/10	40/20	40/40	40/0.794	40/2.5	40/5	40/10	40/20	40/40
$d_{m,i}$ (nm)[a]	172.5	207.7	271.5	311.1	199.3	208.1	185.7	207.7	233.3
$d_{p,f}$ (nm)[a]	146.6	187.7	249	232.7	315.1	316	380.9	557	703.9
X_f (%)[b]	98.07	85.39	53.01	87.52	35.85	24.87	15.22	9.08	5.18
$N_{m,i} \times 10^{-16}$ (1/L)[c]	10.35	5.92	2.65	1.76	6.71	5.89	8.29	5.92	4.18
$N_{p,f} \times 10^{-16}$ (1/L)[d]	14.49	7.05	3.18	3.69	1.61	1.62	0.94	0.3	0.15
$N_{p,f}/N_{m,i}$	1.401	1.19	1.198	2.091	0.24	0.275	0.113	0.051	0.036
n	0.50	0.52	0.59	0.56	0.79	0.80	1.18	3.40	6.77
$nN_{p,f} \times 10^{-16}$ (1/L)	7.31	3.65	1.87	2.08	1.28	1.29	1.11	1.02	1.01
Total scraps (%)	0.33	0.27	0.18	0.13	0.028	0.015	0.006	0.006	0.005

[a] Average monomer droplet diameter immediately before the start of polymerization, determined by DLS.
[b] Final overall conversion.
[c] Initial number of monomer droplets calculated based on the $d_{m,i}$ data.
[d] Final number of latex particles calculated based on the $d_{p,f}$ and X_f data.

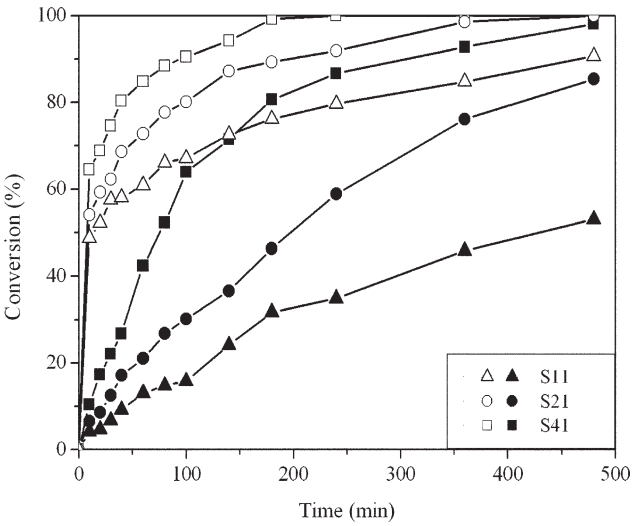

Figure 3 Individual conversions of ST and SMA as a function of time for miniemulsion copolymerizations at 70°C with various mass ratios of ST : SMA. (△, ▲) S11, (○, ●) S21, (□, ■) S41. Open and closed data points represent the individual conversions of SMA and ST, respectively.

radicals in the aqueous phase, f the initiator efficiency factor, k_d the initiator decomposition rate constant, $[I]_w$ the concentration of initiator in water, v_p the volume of a latex particle, k_{tp} the termination rate constant in the latex particles, and N_p the number of latex particles per unit volume of water. The value of f was assumed to be one and k_d and k_{tp}(ST) at 70°C are 2.33×10^{-5} 1/s[34] and 6×10^7 L/mol-s,[35] respectively. The estimated values of n and $nN_{p,f}$ are summarized in Table I. The value of n increases slightly with increasing costabilizer level for the ST/SMA copolymerization system (quite close to the Smith-Ewart Case 2 kinetics), whereas n increases significantly with increasing costabilizer level for the ST/LMA copolymerization system (in the Smith-Ewart Case 3 kinetics region). The product of n and $N_{p,f}$ decreases with increasing SMA level. This trend supports the kinetic data shown in Figure 3; the larger the value of $nN_{p,f}$, the faster the rate of polymerization.

The propagation rate constant at 70°C for the homologous series of alkyl methacrylates in increasing order is: ST (409 L/mol-s[36]) < methyl methacrylate (862[37]) < ethyl methacrylate (1149[36]) < *n*-butyl methacrylate (973[36]) < LMA (1003[36]). It seems reasonable to assume that, for the homologous series of alkyl methacrylates, SMA should have a larger propagation rate constant than MMA. Thus, the propagation rate constant of SMA is expected to be greater than that of ST. The greater the propagation rate constant, the faster the rate of polymerization.

The reactivity ratios of the monomer pair ST/SMA can be estimated by the Finemann–Ross (FR), Inverted Finemann–Ross (IFR), and Kelen–Tudos (KT) methods.[38] First, the FR equation can be written as

$$G = r_m H - r_c, \tag{4}$$

where $G = X(Y-1)/Y$, $H = X^2/Y$, and X and Y are the ratio of the mole fraction of monomer and costabilizer in the feed and the ratio of the mole fraction of monomer and costabilizer in the copolymer, respectively. The parameters r_m and r_c are the reactivity ratios of monomer and costabilizer, respectively. This equation shows that a straight line with a slope of r_m and an intercept of r_c can be obtained when the experimental data of G are plotted versus H [Fig. 5(a)]. The IFR equation is shown as follows:

$$G/H = -r_c(1/H) + r_m \tag{5}$$

By plotting G/H versus $1/H$, as shown in Figure 5(b), the reactivity ratios of ST and SMA can be determined. Finally, the KT equation is shown below.

$$\eta = (r_m + r_c/\alpha)\zeta - r_c/\alpha \tag{6}$$

where $\eta = G/(\alpha + H)$, $\zeta = H/(\alpha + H)$, $\alpha = (H_{\max} \times H_{\min})^{1/2}$ and $H_{\max}$ and $H_{\min}$ are the highest and lowest values of H, respectively. Figure 5(c) (η vs. ζ) represents the KT plot of the miniemulsion copolymerizations of ST and SMA. Multiplying the intercept with α results in the reactivity ratio of SMA. The reactivity ratio of ST can be obtained by subtracting the intercept from the slope.

Based on eq. (4)–6, the reactivity ratios of ST and SMA thus obtained are summarized in Table II. For

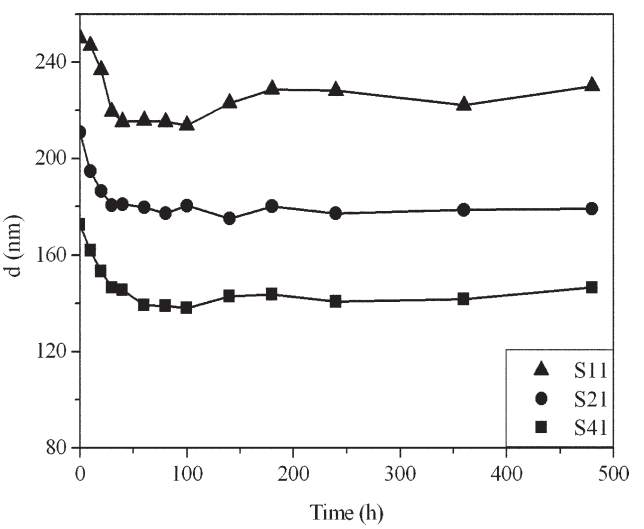

Figure 4 Average colloidal particle diameter as a function of time for miniemulsion copolymerizations at 70°C with various mass ratios of ST : SMA. (▲) S11, (●) S21, (■) S41.

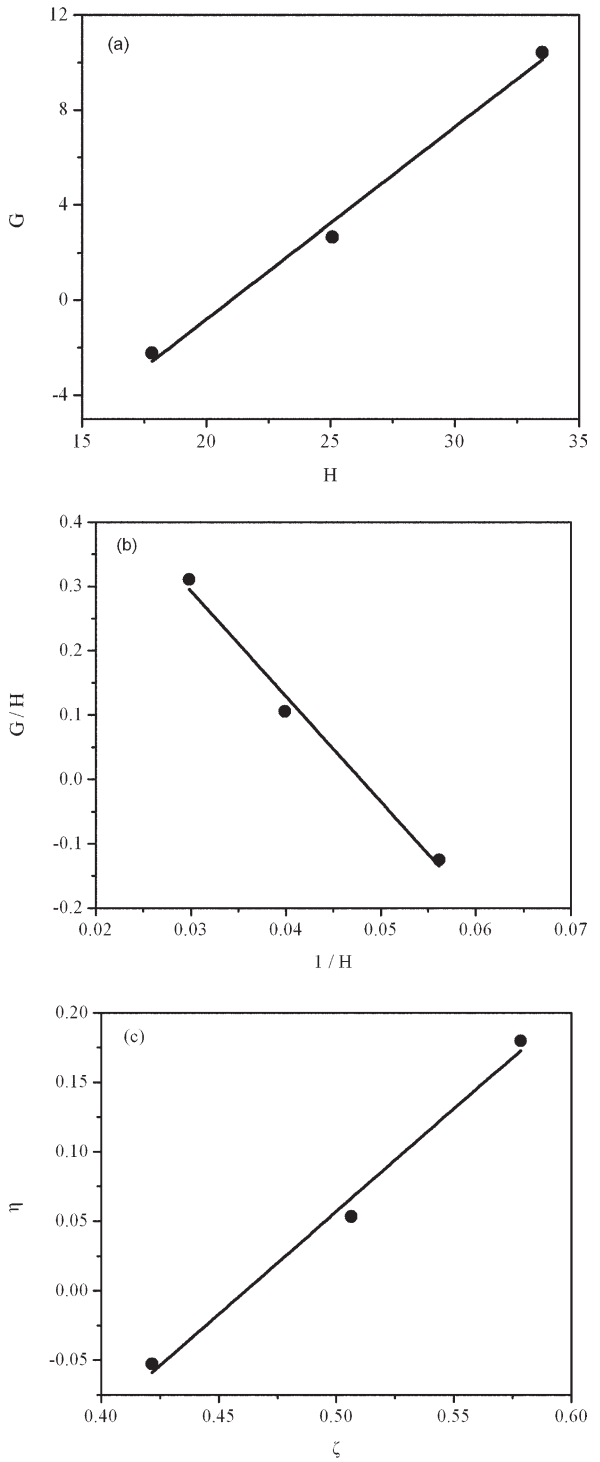

Figure 5 Reactivity ratios of ST and SMA for miniemulsion copolymerizations of ST and SMA. (a) Finemann–Ross plot, (b) Inverted Finemann–Ross plot, and (c) Kelen–Tudos plot.

comparison, the reported reactivity ratios of the monomer pair ST (r_1)/SMA (r_2) for the solution copolymerization system[39] are also included in this table. It is interesting to note that dramatically different reactivity ratios of ST and SMA between the miniemulsion and solution copolymerization systems are obtained. Comparable reactivity ratio values are expected for the solution and ideal miniemulsion copolymerization systems as each monomer droplet can be regarded as a submicron bulk reactor for the free radical copolymerization to take place therein. However, this is not the case. This implies that a mixed mode of particle nucleation (monomer droplet nucleation and homogeneous nucleation) is operative in the miniemulsion copolymerizations of ST and SMA. This postulation is supported by (1) the initial reduction in the size (d) of colloidal particles (including monomer-swollen polymer particles and unnucleated monomer droplets) during polymerization (Fig. 4) and (2) the values of $N_{p,f}/N_{m,i}$ greater than one, where $N_{p,f}$ and $N_{m,i}$ are the final number of latex particles and initial number of monomer droplets per unit volume of water, respectively.

A general feature of the d versus t profiles is that the average colloidal particle size first decreases to a minimum and then increases gradually to a plateau (Fig. 4). The initial decrease of d is attributed to the formation of tiny particle nuclei (ca. 10° nm in diameter) in the continuous aqueous phase.[19] Micellar nucleation can be ruled out because the SLS concentration used in this work is below its CMC. Under the circumstance, the average colloidal particle size starts to decrease from the very beginning of polymerization and, ultimately, the ratio $N_{p,f}/N_{m,i}$ is greater than unity. Homogeneous nucleation stops and a minimal value of d is achieved when the total particle surface area is large enough to capture all the oligomeric radicals generated in water. This is

TABLE II
Average Reactivity Ratio Data Predicted by Finemann–Ross, Inverted Finemann–Ross and Kelen–Tudos Plots for miniemulsion copolymerization Systems with ST/SMA and ST/LMA

	r_1[a]	r_2[b]	$r_1 - r_2$
P(ST-*co*-SMA)[c]			
FR	1.799	0.674	1.212
invFR	1.734	0.548	0.950
KT	1.758	0.510	0.896
P(ST-*co*-SMA)[d]			
FR	0.809	16.981	13.731
invFR	0.783	16.353	12.806
KT	0.796	16.655	13.251
P(ST-*co*-LMA)[e]	0.57	0.45	0.26
P(ST-*co*-LMA)[d]			
FR	0.092	9.331	0.862
invFR	0.100	11.375	1.141
KT	0.053	7.317	0.387

[a] Reactivity ratio of ST.
[b] Reactivity ratio of SMA or LMA.
[c] Prepared by solution polymerization.[39]
[d] Prepared by miniemulsion copolymerization in this work.
[e] Prepared by bulk polymerization.[36]

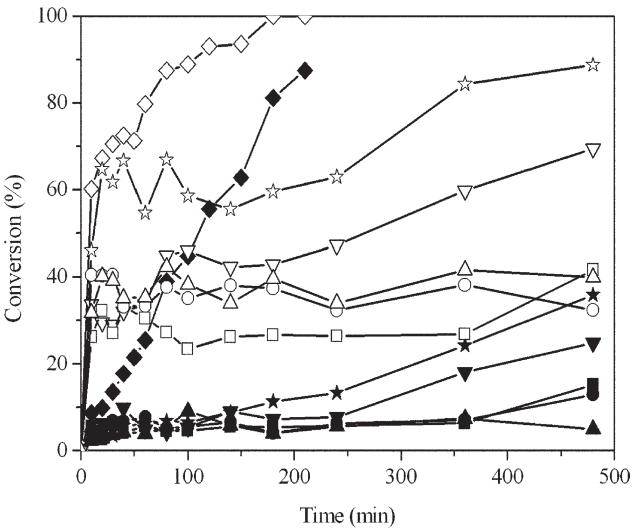

Figure 6 Individual conversions of ST and LMA as a function of reaction time for miniemulsion copolymerizations at 70°C with various mass ratios of ST : LMA. (△, ▲) L11, (○, ●) L21, (□, ■) L41, (▽, ▼) L81, (☆, ★) L161, (◇, ◆) L501. Open and closed data points represent the individual conversions of LMA and ST, respectively.

followed by the slow growth of the particles by acquiring monomer molecules from unnucleated monomer droplets. It is noteworthy that the particles originating from homogeneous nucleation do not contain any SMA species because the extremely hydrophobic SMA molecules cannot diffuse from monomer droplets or particles originating from monomer droplet nucleation, across the aqueous phase, into the water-borne particle nuclei. As a result, the apparent reactivity ratios of ST and SMA for the miniemulsion copolymerization system are quite different from those obtained from the solution copolymerization system. All these factors (i.e., the number of reaction loci per unit volume of water, the propagation rate constant and the apparent reactivity ratios of ST and SMA for the miniemulsion copolymerizations of ST and SMA) support the kinetic behavior observed in Figure 3.

In contrast to the ST/SMA series, miniemulsions with various mass ratios of ST to LMA all exhibit significant Ostwald ripening and the Ostwald ripening rate decreases with increasing LMA concentration [Figs. 1(b,c) and 2]. This is as would be expected since LMA (water solubility = 1.38×10^{-8} cm^3/cm^3)[5] is not as effective as the extremely hydrophobic SMA (water solubility = 3.23×10^{-9} cm^3/cm^3)[5] in retarding the diffusional degradation of monomer droplets (Ostwald ripening). Figure 6 shows the individual conversions of ST and LMA as a function of time for miniemulsion copolymerizations of ST and LMA with various levels of LMA at 70°C. Similar to the monomer pair ST/SMA, the rate of polymerization of LMA is much faster than that of ST regardless of the LMA concentration. As expected, the larger propagation rate constant[36] and reactivity ratio of LMA (Table II) compared with those of ST are responsible for such a polymerization kinetic behavior. In addition, the decreased value of $nN_{p,f}$ with LMA level also contributes to some extent to the observed kinetic behavior in Figure 6.

The average colloidal particle size (d) versus time profiles for miniemulsion copolymerizations of ST and LMA are shown in Figure 7. All the curves exhibit a general feature that the average colloidal particle size increases continuously (for the runs with mass ratios of ST : LMA = 2 : 1, 1 : 1) or first increases and then levels off (for the runs with ST : LMA = 16 : 1, 8 : 1, 4 : 1) with the progress of polymerization except the run with ST : LMA = 50.4 : 1. This is most likely because of the significant Ostwald ripening effect experienced in miniemulsions comprising ST and LMA. For the run with a mass ratio of ST : LMA = 50.4 : 1 that shows the strongest Ostwald ripening effect, the average colloidal particle size first decreases rapidly to a minimum and then increases toward the end of polymerization. The rapidly decreased average colloidal particle size with time implies that formation of particle nuclei in water plays an important role in the polymerization system and the effect of homogeneous nucleation is not overridden by that of Ostwald ripening. It should be noted that the value of $N_{p,f}/N_{m,i}$ is smaller than one for the run with ST : LMA = 50.4 : 1 (Table I). Considering the initial decrease of d and the value of $N_{p,f}/N_{m,i}$ smaller than unity, monomer droplet nucleation should be relatively weak compared to homogeneous nucleation. Thus, monomer droplet nucleation seems to be retarded severely by Ostwald

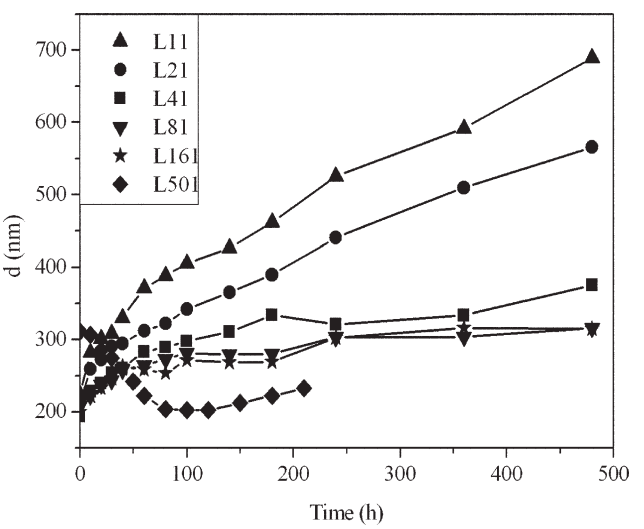

Figure 7 Average colloidal particle diameter as a function of time for miniemulsion copolymerizations at 70°C with various mass ratios of ST : LMA. (▲) L_{11}, (●) L_{21}, (■) L_{41}, (▼) L_{81}, (★) L_{161}, (◆) L_{501}.

ripening. It was reported that a significant fraction of latex particles were generated by homogeneous nucleation for the LMA containing miniemulsion polymerization system, which exhibited a strong Ostwald ripening effect.[28,40–42] Thus, formation of water-borne particle embryos cannot be ruled out for the runs with the mass ratios of ST : LMA = 16 : 1, 8 : 1, 4 : 1, 2 : 1, 1 : 1, though the absence of the initial reduction in the average colloidal particle size is evident (Fig. 7). This is because the extent of homogeneous nucleation decreases with increasing LMA concentration. Under the circumstance, the Ostwald ripening effect is so strong that formation of particle nuclei in the aqueous phase during the early stage of polymerization cannot be detected by the DLS technique except the run with ST : LMA = 50.4 : 1 exhibiting the strongest homogeneous nucleation. The fact that all the values of $N_{p,f}/N_{m,i}$ are smaller than one implies that monomer droplet nucleation is greatly retarded because of the strong Ostwald ripening effect experienced in miniemulsion copolymerizations of ST and LMA. As a consequence, relatively slow rates of copolymerizations of ST and LMA were attained compared with the ST/SMA counterpart. Furthermore, the extent of the retarded particle nucleation (including monomer droplet nucleation and homogeneous nucleation) increases with increasing LMA concentration, as shown by the decreased $N_{p,f}/N_{m,i}$ with increasing LMA in Table I. Thus, the final overall conversion decreases with increasing LMA concentration.

CONCLUSIONS

Miniemulsion copolymerizations of styrene (ST) and alkyl methacrylates (including stearyl methacrylate (SMA) and lauryl methacrylate (LMA)) were investigated. The miniemulsions comprising ST and various levels of SMA upon aging at 30°C showed very good stability against the diffusional degradation of monomer droplets (Ostwald ripening), whereas miniemulsions comprising ST and various levels of LMA exhibited significant Ostwald ripening. The Ostwald ripening first decreases and then levels off when the level of LMA is increased. This is attributed to the more hydrophobic SMA that acts as a very effective reactive costabilizer in stabilizing the ST miniemulsions.

In miniemulsion copolymerizations of ST and SMA, in which Ostwald ripening was greatly retarded, particle nucleation occurring in the continuous aqueous phase (homogeneous nucleation) plays an important role in addition to monomer droplet nucleation. The final overall conversion and the individual conversions of ST and SMA all decrease with increasing SMA concentration. This is caused by the decreased number density of particle nuclei (i.e., reaction loci) with the SMA concentration. Furthermore, at a particular reaction time, the conversion of SMA is always greater than that of ST, and the difference between the individual conversions of ST and SMA increases with increasing SMA concentration. This can be explained by the larger propagation rate constant and reactivity ratio of SMA than those of ST. The significant Ostwald ripening experienced in miniemulsion copolymerizations of ST and LMA had a significant influence on the copolymerization mechanisms and kinetics. Monomer droplet nucleation was retarded significantly for the monomer pair ST/LMA. As a result, relatively slow rates of copolymerizations of ST and LMA were attained compared with the ST/SMA counterpart. Moreover, the extent of the retarded particle nucleation (including monomer droplet nucleation and homogeneous nucleation) increases with increasing LMA concentration. This will then result in the decreased $N_{p,f}/N_{m,i}$ with LMA concentration. Thus, the final overall conversion decreases with increasing LMA concentration.

References

1. Landfester, K. Macromol Rapid Commun 2001, 22, 896.
2. Highuci, W. I.; Misra, J. J Pharm Sci 1962, 51, 459.
3. Choi, Y. T. Formation and stabilization of miniemulsion and latexes, PhD Dissertation, Lehigh University, Bethlehem, 1986.
4. Kabalnov, A. S.; Makarov, K. N.; Pertzov, A. V.; Shchukin, E. D. J. Colloid Interface Sci 1990, 138, 98.
5. Chern, C. S.; Chen, T. J. Colloids Surf A 1998, 138, 65.
6. Tauer, K. Polymer 2005, 46, 1385.
7. Harkins, W. D. J Chem Phys 1945, 13, 381.
8. Harkins, W. D. J Chem Phys 1946, 14, 47.
9. Harkins, W. D. J Am Chem Soc 1947, 69, 1428.
10. Smith, W. V. J Am Chem Soc 1948, 70, 3695.
11. Smith, W. V.; Ewart, R. H. J Chem Phys 1948, 16, 592.
12. Smith, W. V. J Am Chem Soc 1949, 71, 4077.
13. Priest, W. J. J Phys Chem 1977, 56, 1977.
14. Roe, C. P. Ind Eng Chem 1968, 60, 20.
15. Fitch, R. M.; Tsai, C. H. Polymer Colloids, Fitch, R. M., Ed.; Plenum Press: New York, 1971; p 73.
16. Fitch, R. M.; Tsai, C. H. Polymer Colloids, Fitch, R. M., Ed.; Plenum Press: New York, 1971; p 103.
17. Fitch, R. M. Br Polym J 1973, 5, 467.
18. Ugelstad, J.; El-Aasser, M. S.; Vanderhoff, J. W. J Polym Sci: Polym Lett Ed 1973, 11, 503.
19. Ugelstad, J.; Hansen, F. K.; Lange, S. Die Makromol Chem 1974, 175, 507.
20. Durbin, D. P.; El-Aasser, M. S.; Poehlein, G. W.; Vanderhoff, J. W. J Appl Polym Sci 1979, 24, 703.
21. Chamberlain, B. J.; Napper, D. H.; Gilbert, R. G. J Chem Soc Faraday Trans 1 1982, 78, 591.
22. Choi, Y. T.; El-Aasser, M. S.; Sudol, E. D.; Vanderhoff, J. W. J Polym Sci: Polym Chem Ed 1985, 23, 2973.
23. Capek, I.; Chern, C. S. Adv Polym Sci 2001, 155, 101.
24. Antonietti, M.; Landfester, K. Prog Polym Sci 2002, 27, 689.
25. Asua, J. M. Prog Polym Sci 2002, 27, 1283.
26. Chern, C. S.; Chen, T. J. Colloid Polym Sci 1997, 275, 546.
27. Chern, C. S.; Chen, T. J. Colloid Polym Sci 1997, 275, 1060.
28. Chern, C. S.; Liou, Y. C. Polymer 1999, 40, 3763.
29. Chern, C. S.; Sheu, J. C. Polymer 2001, 42, 2349.

30. Chern, C. S.; Lin, C. T.; Shiau, F. T. Colloid Polym Sci 2009, 287, 1139.
31. Kabalnov, A. S.; Shchukin, E. D. Adv Colloid Interface Sci 1992, 38, 69.
32. Rehfeld, S. J. J Phys Chem 1967, 71, 738.
33. Ugelstad, J.; Mork, P. C. Br Polym J 1970, 2, 31.
34. Brandrup, J.; Immergut, E. H. Polymer Handbook; 3rd ed; Wiley, New York, 1989.
35. Tobolsky, A. V.; Rogers, C. E.; Brickman, R. D. J Am Chem Soc 1960, 82, 1277.
36. Davis, T. P.; Driscoll, K. F.; Piton, M. C.; Winnik, M. A. Macromolecules 1990, 23, 2113.
37. Mahabadi, H. K.; O'driscoll, K. F. J Macromol Sci Chem 1997, 11, 967.
38. Ziaee, F.; Nekoomanesh, M. Polymer 1998, 39, 203.
39. Stergiou, G.; Dousikos, P. P. Eur Polym J 2002, 38, 1963.
40. Chern, C. S.; Chen, T. J.; Liou, Y. C. Polymer 1998, 39, 3767.
41. Chern, C. S.; Liou, Y. C. Macromol Chem Phys 1998, 199, 2051.
42. Chern, C. S.; Liou, Y. C. J Polym Sci Polym Chem Ed 1999, 37, 2537.